

Richard Feynman

“There’s Plenty of Room at the Bottom” (1959)

Talk given at the annual meeting of the APSociety at the California Institute of Technology

But I am not afraid to consider the final question as to whether, ultimately - in the great future - we can arrange the atoms the way we want; the very atoms, all the way down! What would happen if we could arrange the atoms one by one the way we want them (within reason, of course; you can't put them so that they are chemically unstable, for example). (...)

What could we do with layered structures with just the right layers? What would the properties of materials be if we could really arrange the atoms the way we want them? They would be very interesting to investigate theoretically. I can't see exactly what would happen, but I can hardly doubt that when we have some control of the arrangement of things on a small scale we will get an enormously greater range of possible properties that substances can have, and of different things that we can do.

His visionary talk covered a wide range of concepts and promises, on which we work today in the meanwhile established field of nanoscience.

For example, he pointed out

- the close relationship of physics and biology when it comes to Nanostructures
- the importance of quantum effects in structures built from a few atoms

His ideas of how to produce nanometer-size structures included

- thin-film evaporation through masks, somehow predicting today's experiments with two-dimensional electron gases.
- a series of machines of decreasing length scale, each generation constructing the next smaller one.

This extensive approach has been outrun by a simpler solution:

With the invention of Scanning Probe Microscopy the large gap between the macroscopic world and single atom manipulation has been bridged in one step.

Scanning Probe Microscopy (SPM)

- covers a lateral range of imaging from several 100 μm to 100 pm
- Surfaces of solids can be resolved with atomic resolution,
 - revealing not only the structure of perfect crystalline surfaces
 - the distribution of point defects, adsorbates,
 - structural defects like steps
- has become an essential tool in the emerging field of nanoscience,
- local experiments on single atoms or molecules can be performed
- force measurements of single chemical bonds or optical spectra of single molecules can be performed
- local probe can be used to manipulate single atoms or molecules and hence to form artificial structures on atomic scale.

Scanning Probe Microscopy Family

- The starting point of SPM was the invention of the *Scanning Tunneling Microscope* (STM) by G. Binnig and H. Rohrer in 1982 [1,2] (Nobel prize in physics in 1986).

The family present family of scanning probe microscopes is based on a variety of tip-sample interactions:

- The first and most important extension of the STM was the scanning force microscope (SFM) or atomic force microscope (AFM), invented in 1986 by Binnig, Quate, and Gerber [3].
- The third distinguished member of the family of SPMs is the scanning near-field optical microscope (SNOM), which uses short-ranged components of the electromagnetic field as tip-sample interaction.

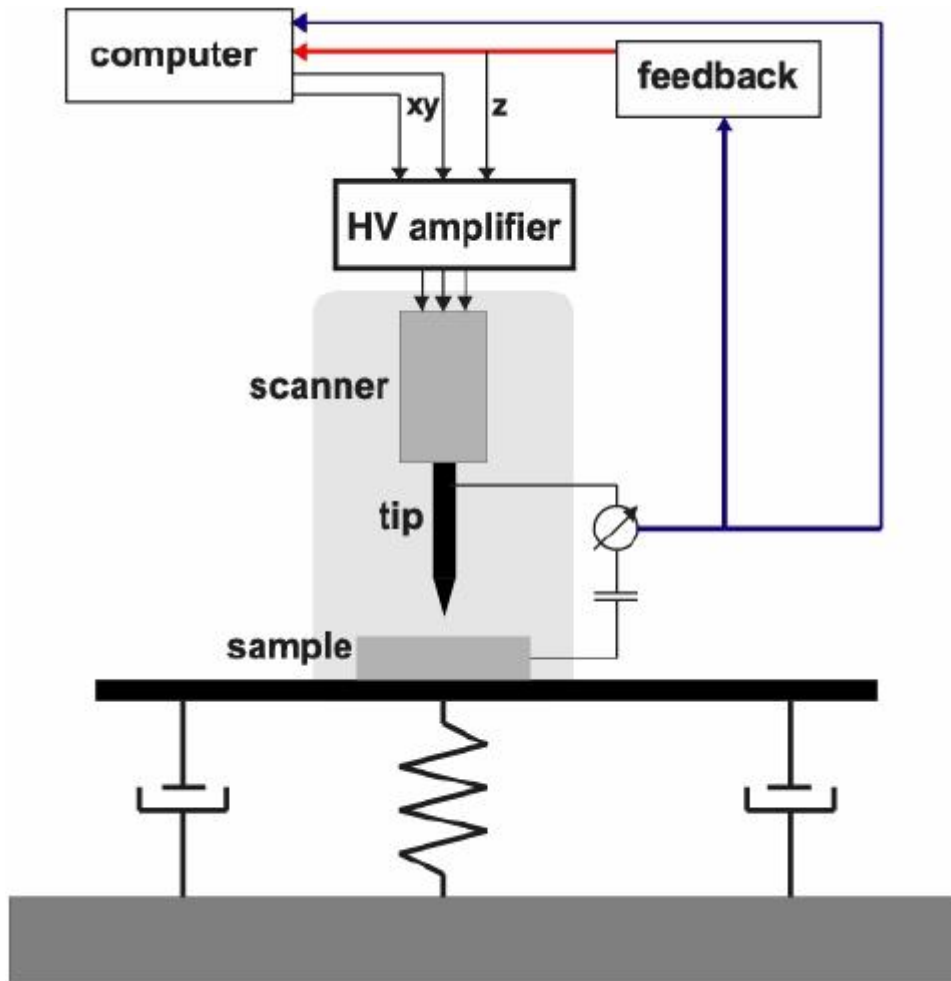
[1] G. Binnig and H. Rohrer et al. Helv. Phys. Acta 55, 726 (1982)

[2] G. Binnig and H. Rohrer et al. Phys. Rev. Lett. 50, 120 (1983)

[3] G. Binnig, C.F. Quate, CH. Gerber, Phys. Rev. Lett. 56, 930 (1986)

Basic Concepts of an Scanning Tunneling Microscopy (STM)

Basic setup of an STM



-good vibration isolation of the experiment is prerequisite for high-resolution imaging

-the mechanical stability of the experimental setup turns out to be a prerequisite for successful measurements on the atomic scale

-the tip is moved in three dimensions by piezoelectric actuators

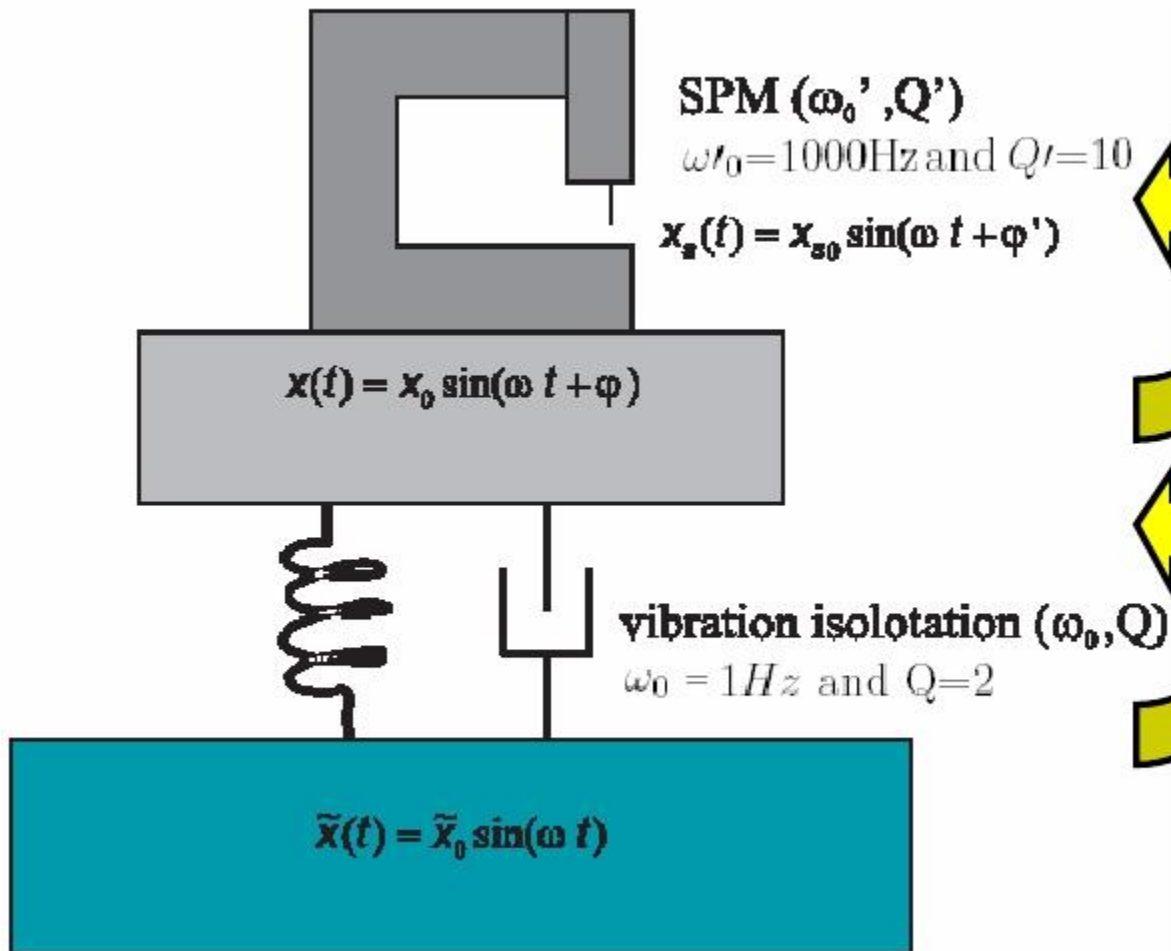
-a high-voltage amplifier is required to drive the piezoelectric scanner

-the tunneling current is used to control the tip-sample distance z via a feedback circuit that keeps the tunneling current constant

- the distance z is recorded by a computer as function of the scanned coordinates x,y

In an STM typically two signals are acquired, namely the z -coordinate (topography) and the tunneling current (error signal)

Vibration Isolation

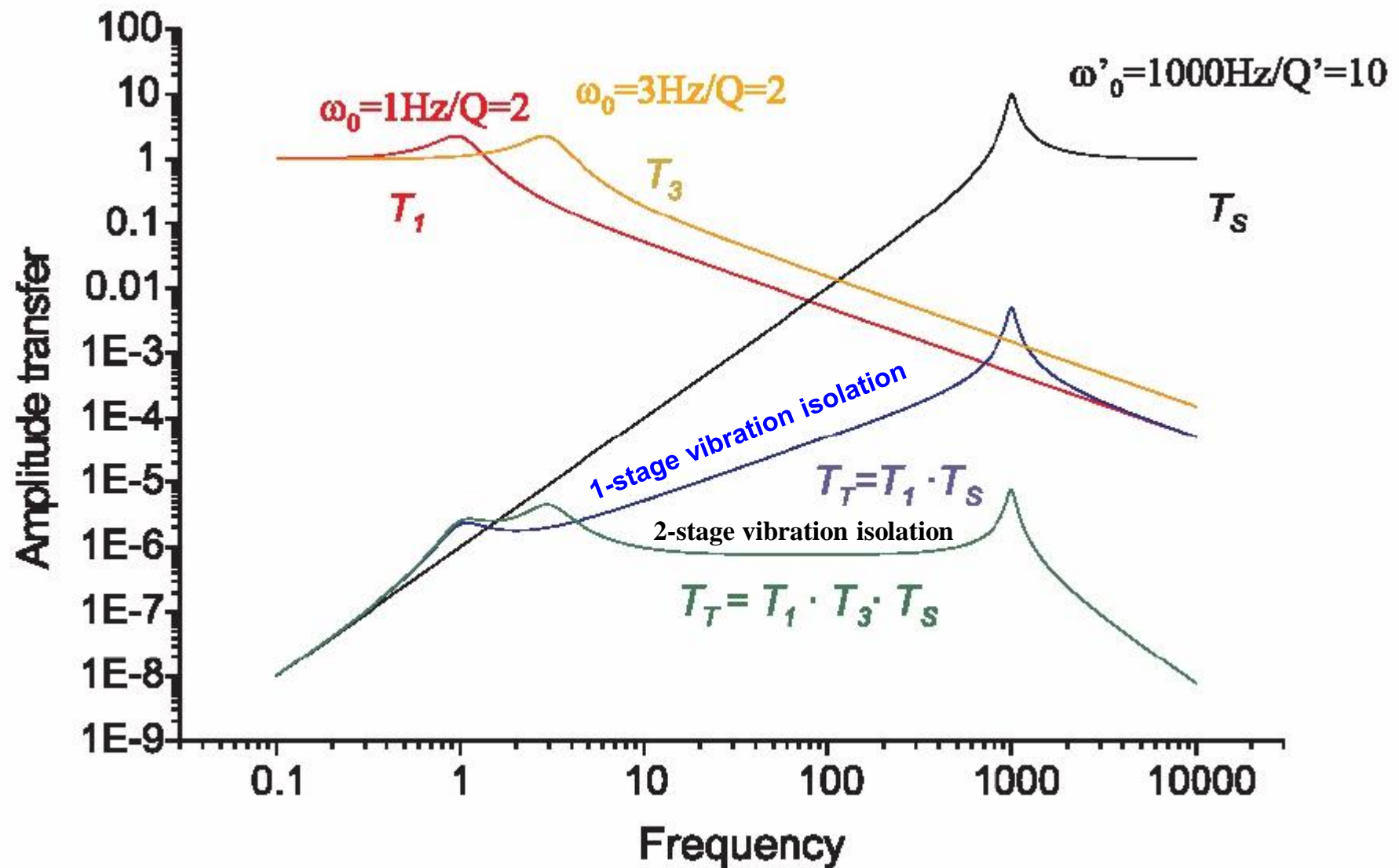


$$T_T = T \cdot T_S \quad \text{total transfer}$$

$$T_S = \frac{|x_{s0}|}{|x_0|} = \frac{\left(\frac{\omega}{\omega'_0}\right)^2}{\sqrt{\left(1 - \left(\frac{\omega}{\omega'_0}\right)^2\right)^2 + \left(\frac{\omega}{Q'\omega'_0}\right)^2}}$$

$$T = \frac{|x_0|}{|\tilde{x}_0|} = \sqrt{\frac{1 + \left(\frac{\omega}{Q\omega_0}\right)^2}{\left(1 - \left(\frac{\omega}{\omega_0}\right)^2\right)^2 + \left(\frac{\omega}{Q\omega_0}\right)^2}}$$

One & Two Stage Vibration Isolation

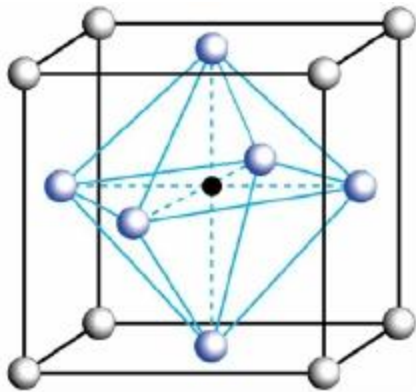


Only the double vibration isolation stage can provide sufficient isolation @ the resonance frequency of the microscope. Assume floor vibrations of 100 nm (1KHz). Then the tip-sample vibration will be less than 10⁻³nm.

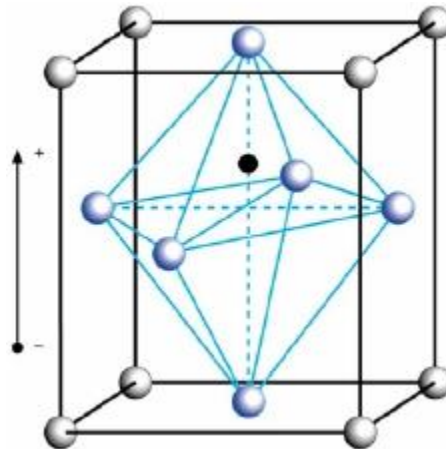
Piezo Electric Actuators

Since the piezo effect exhibited by natural materials (e.g. quartz) is very small, polycrystalline ferroelectric ceramic materials such as barium titanate and lead zirconate titanate (PZT) with improved properties (e.g. PZT-5H: $d_{31} = -2.62 \text{ \AA/V}$) have been developed. These ferroelectric ceramics become piezoelectric when poled.

$T > T_c$
cubic crystal structure



$T < T_c$
tetragonal crystal structure



$$\Delta L = d_{31} \cdot L \cdot \vec{E}$$

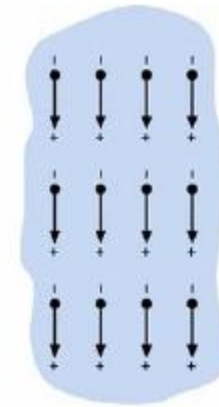
→

E electric field, L lengths, ΔL change in length
 d_{31} transversal piezoelectric coefficient

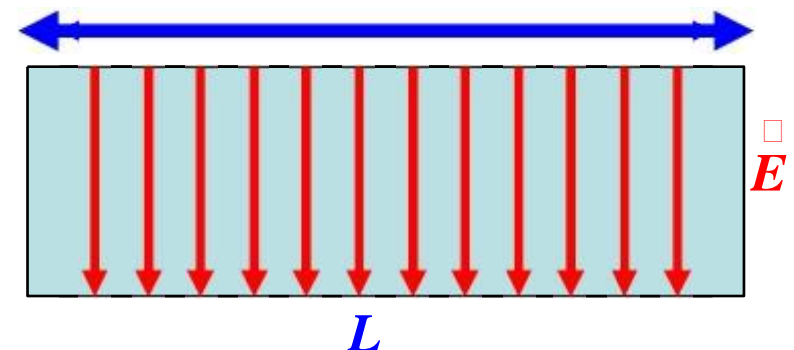
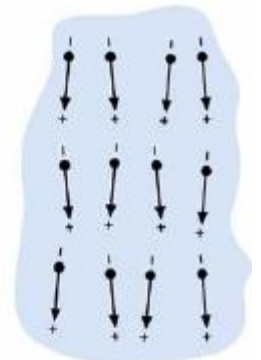
depolarized
Ferroelectric
structure



during
polarization

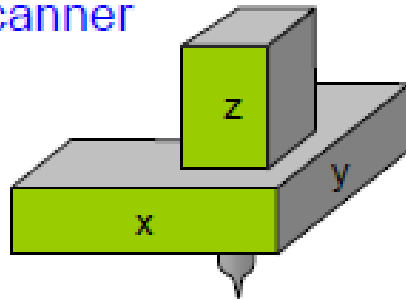


after
polarization

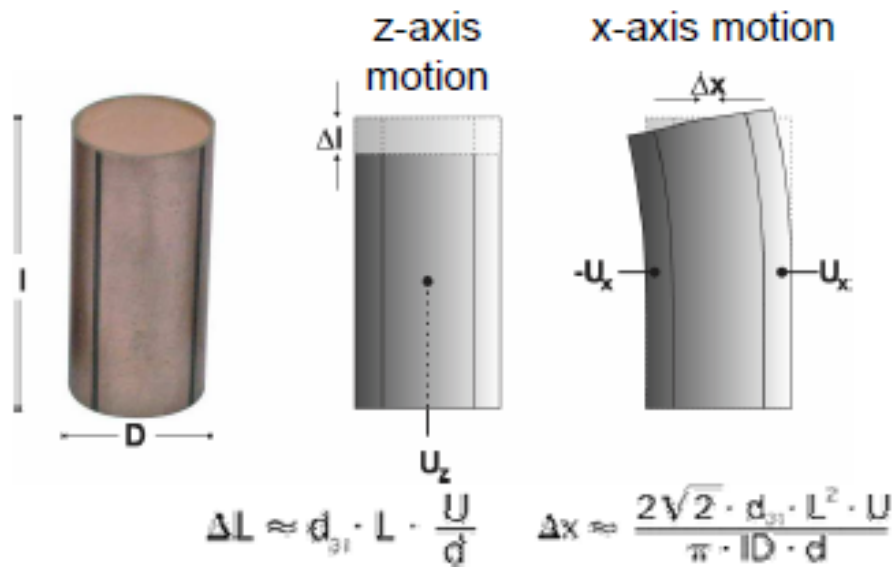


Piezo Electric Nanopositioners

tripod scanner



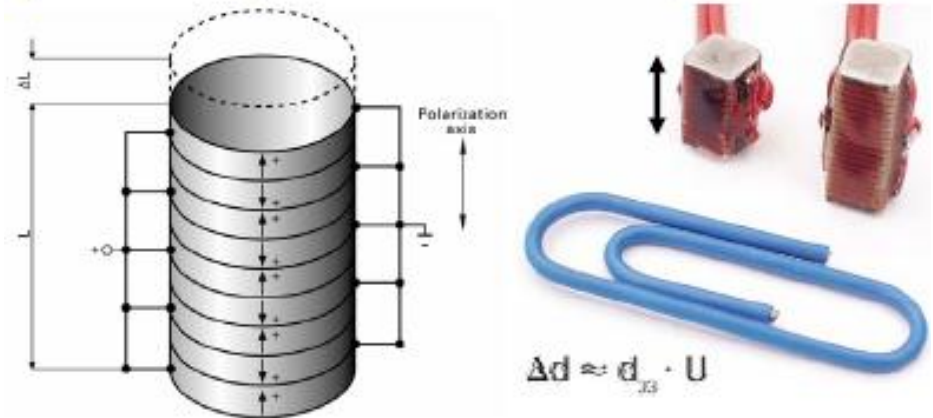
tube scanner (4 outer, 1 inner electrode)



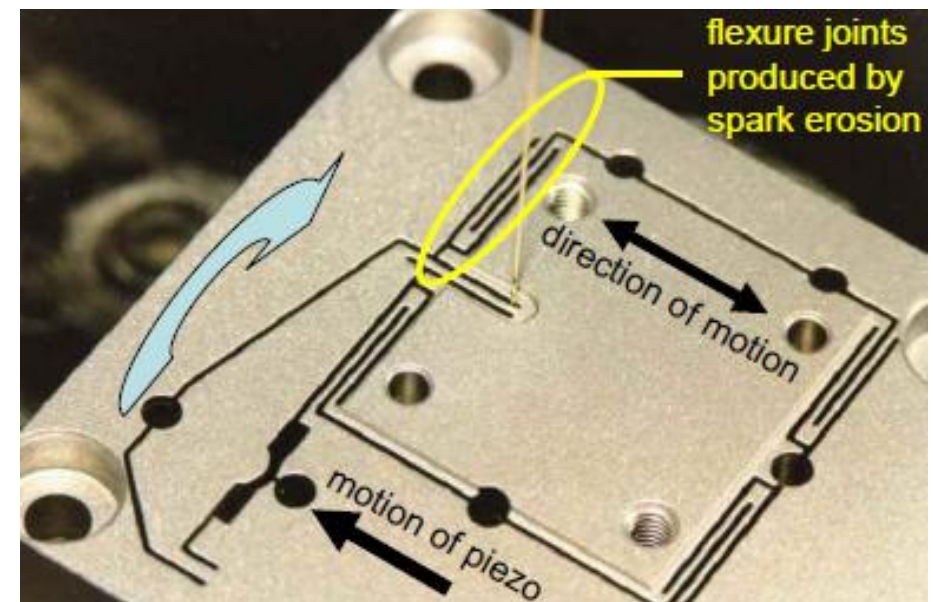
L: length
ID: inner diameter
U: applied voltage
 d_{31} : transversal piezo constant
 d_{33} : longitudinal piezo constant

D: diameter
d: wall thickness

piezo stacks (linear or shear motion)

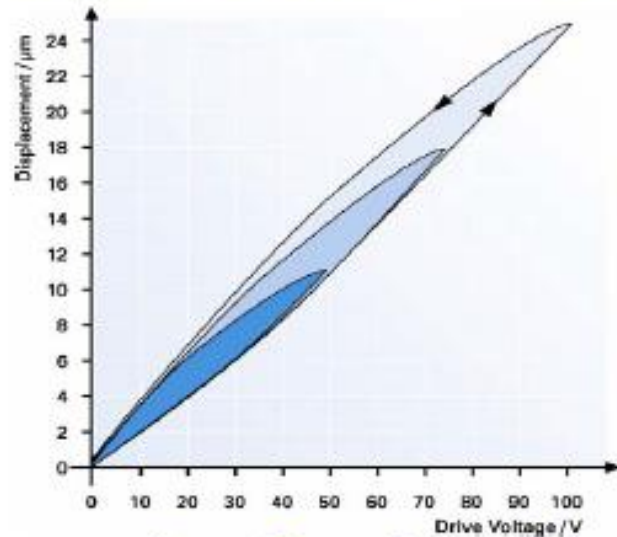


piezo flexure nanopositioners

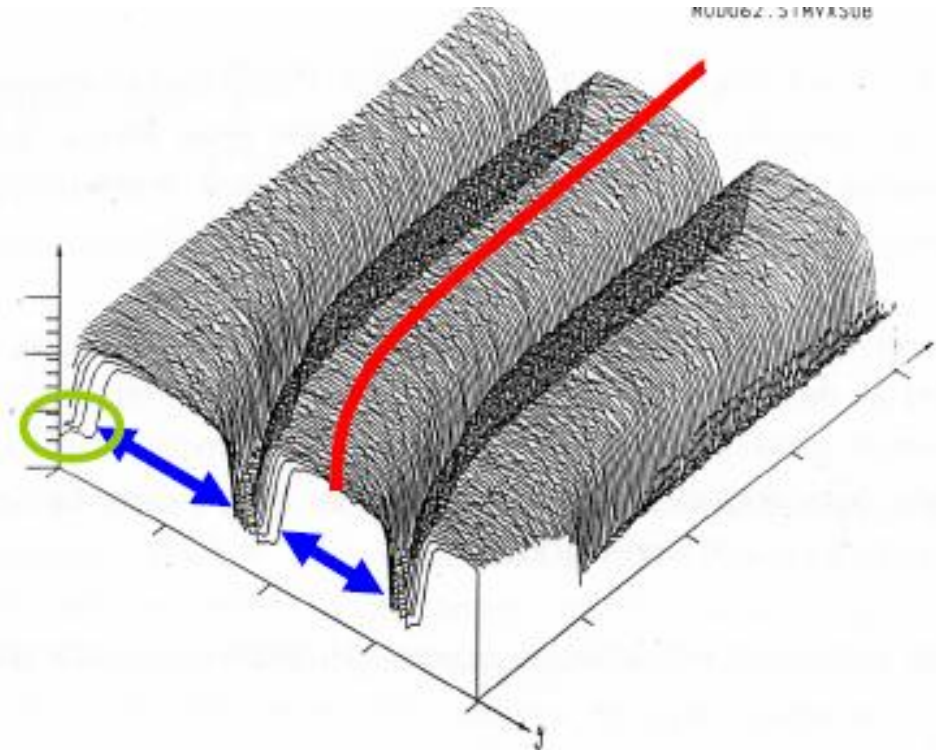
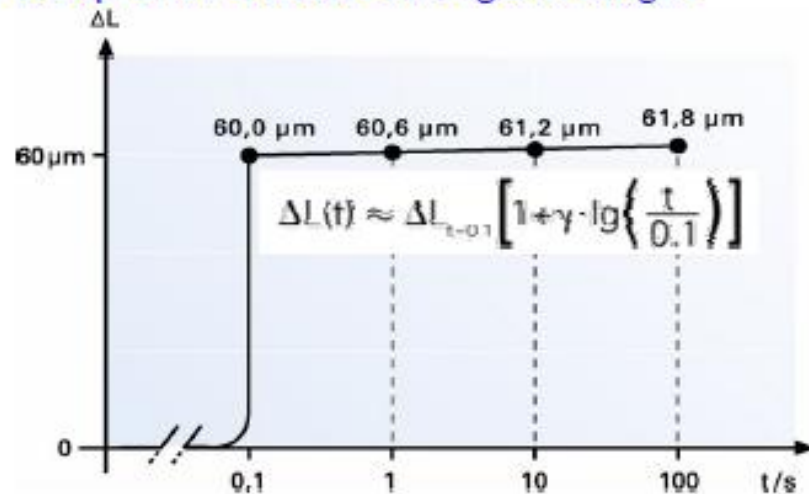


Hysteresis and Creep

hysteresis for various peak voltages



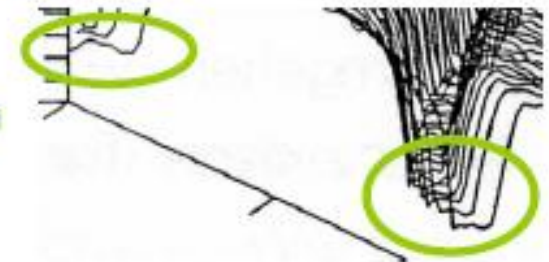
creep after a 60 μm change in length



scan distortions due to piezo creep

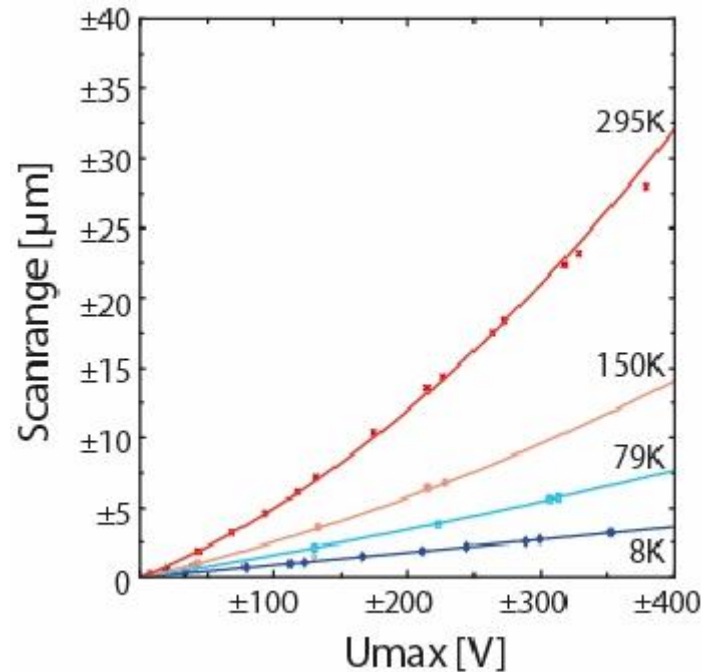
- increase of apparent sensitivity
- distortion in y-direction

- creep in z-direction



Temperature Effects & Hysteresis and Creep Correction

piezo sensitivity at various temperatures



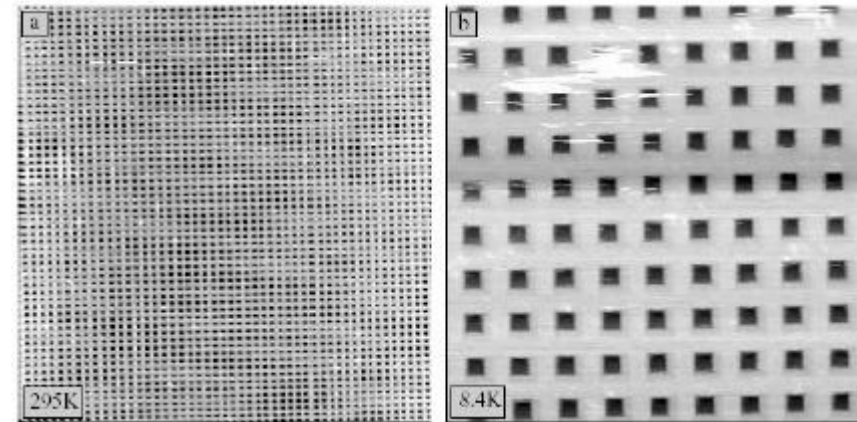
- quadratic dependence of range on maximal voltage

$$d(U_{max}, t_{Scan}, T) = \alpha \cdot U_{max} + \beta \cdot U_{max}^2$$

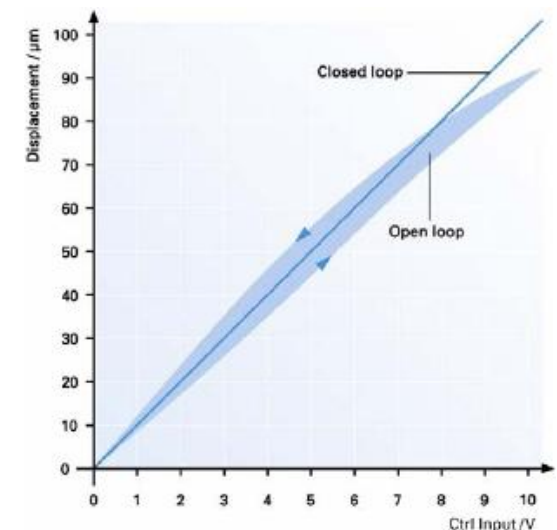
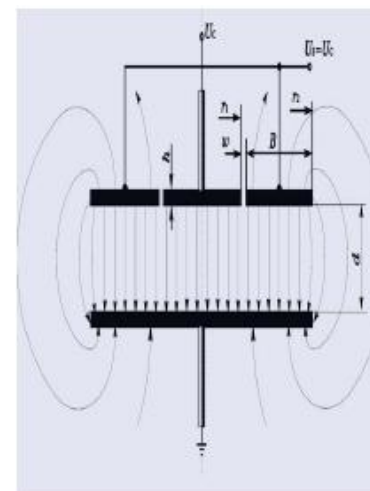
- extremely small creep @ 8K but:
- about ten-fold decreased piezo sensitivity at 8K

creep correction by sub-linear scanning

$$U(t, d, t_{Scan}, T) = \frac{\alpha + \sqrt{\alpha^2 + 4\beta d}}{2\beta} \cdot \left(\frac{t}{t_{Scan}}\right)^\gamma$$

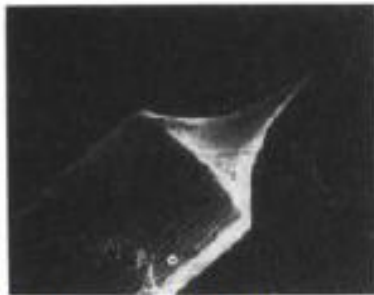


closed loop piezo motion with position sensor

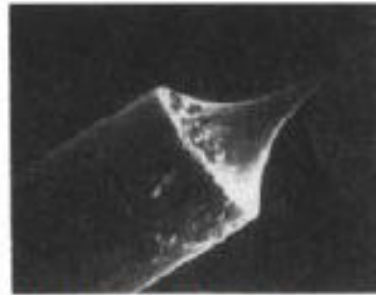


Tunneling Tips

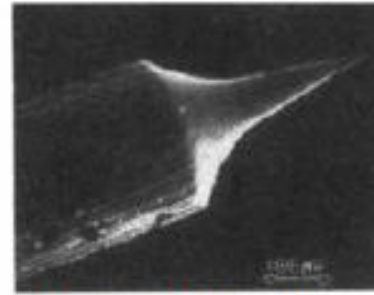
- Electrochemical etching:
 - a 0.25mm tungsten wire is immersed in 1M aqueous solution of NaOH.
 - the counterelectrode is a piece of stainless steel or platinum
 - a positive voltage of 4-12V is applied to the wire.
 - etching occurs at the liquid-air interface and a neck is formed
 - the weight of the lower part of the wire pulls the neck and naturally fractures it.
 - cutoff time after the tip has fractured is important parameter
 - cleaning in boiling water to remove residuals of NaOH.
 - problem: formation of a surface oxide during etching, which has to be removed before tunneling
 - remove the oxide by resistive heating or electron bombardment
- Mechanical methods: cut PtIr wire with scissors !
- Field evaporation: in combination with FIM atomically sharp tips
- Controlled collision with surface



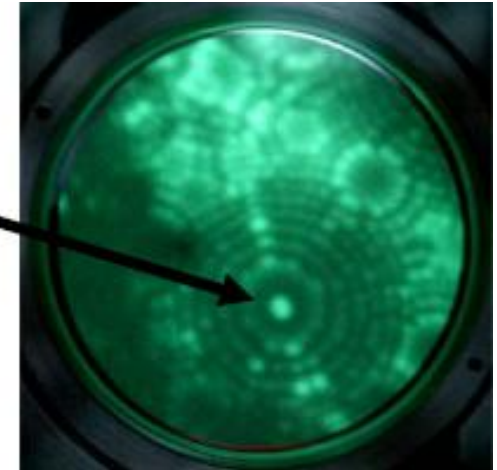
600ns, with 32nm



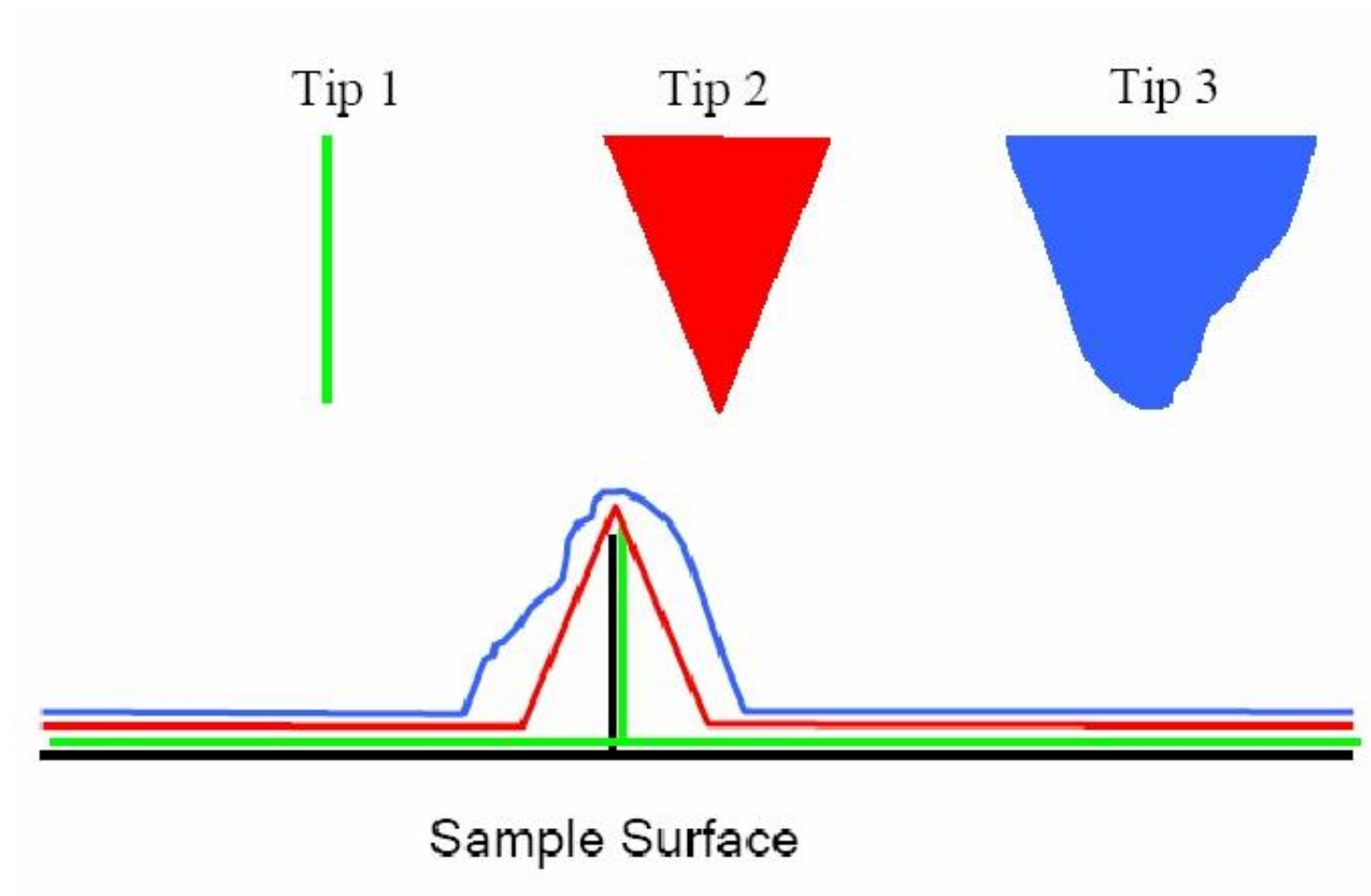
140ms, with 58nm



640ms, with 100nm.



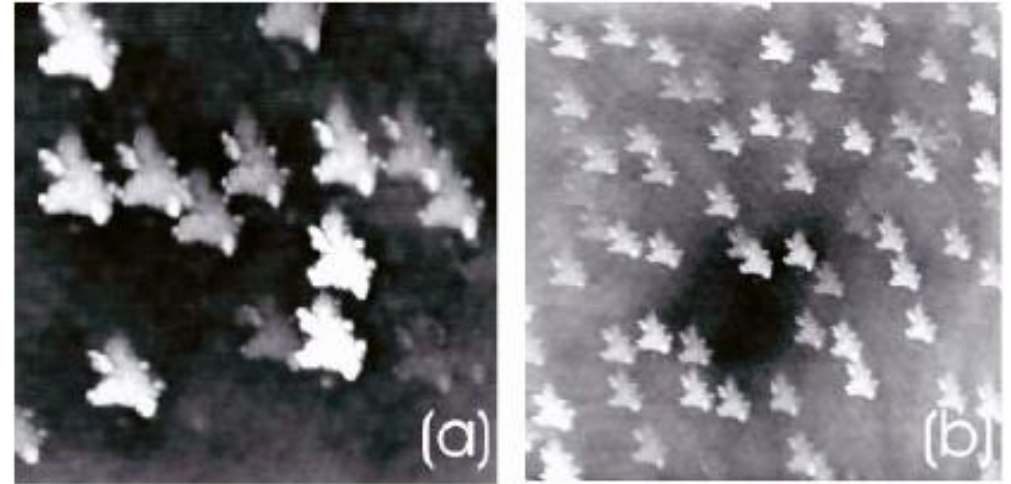
Influence of the Tip Geometry on Imaging Surface Features



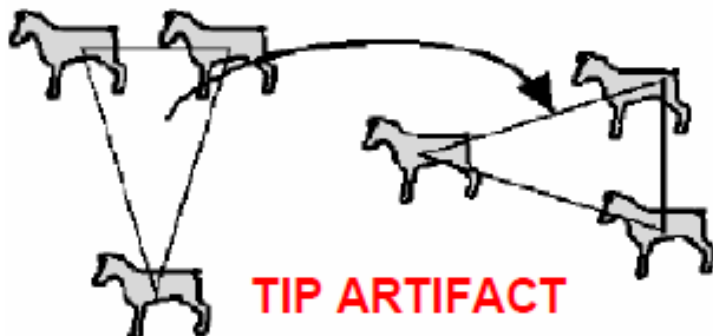
Tip Shape Artifacts

The image of a sample with needle-like structures (here an Al_2O_3 surface imaged by AFM) shows tip artifacts. The (blunter) tip is imaged by the sharp(er) needle-like structures existing on the sample.

A conclusive but sometimes difficult to realize test is to compare images of the (same) sample (area) before and after a 90 degree the rotation of the sample.



Features of the image DO NOT rotate



Features of the image DO rotate



Calibration of Tip-Shape

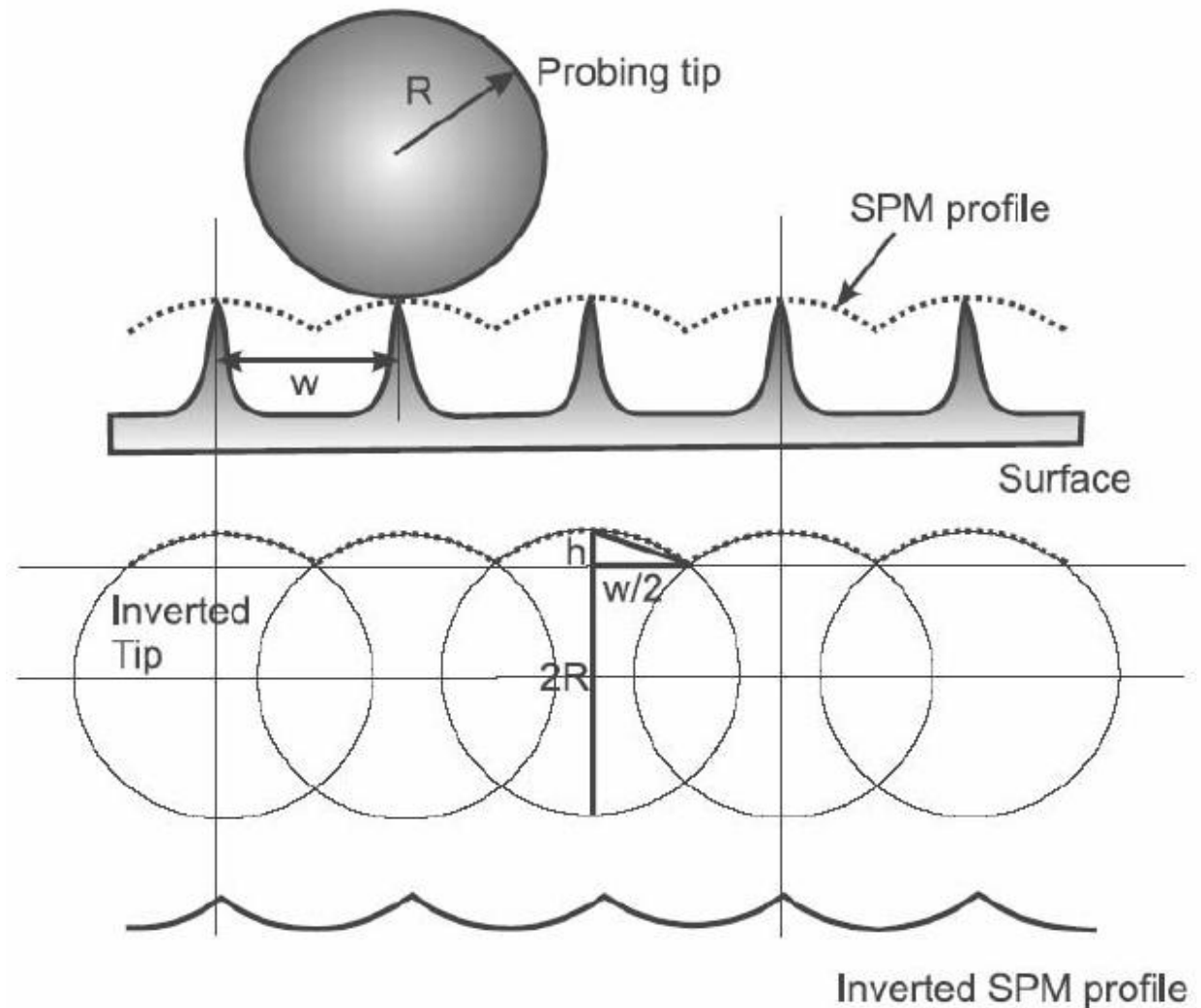


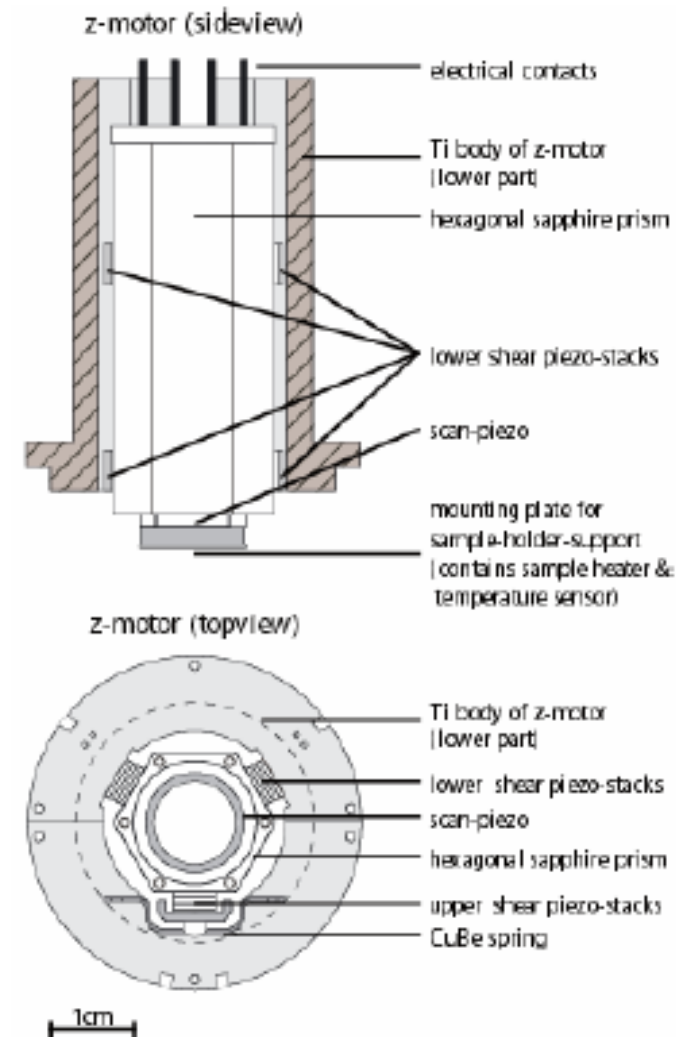
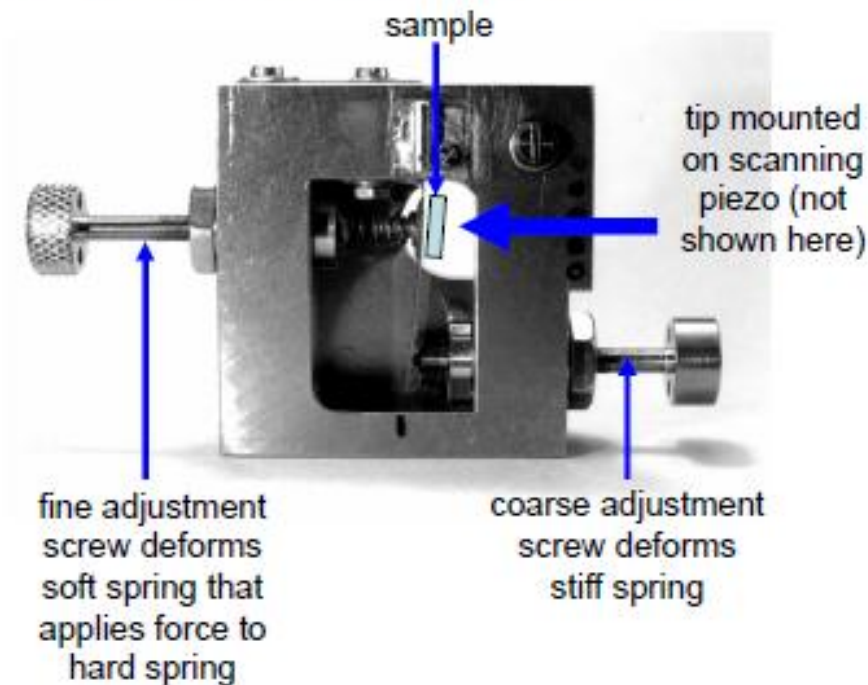
Fig. 6.3. The SPM profile of narrowly spaced holes is dominated by the inverted tip images, which are spaced by the hole dimension, w . The observed corrugation height is reduced, because the tip can not reach the bottom of the holes. Also, the SPM profile does not appear as holes, but as hillocks with a curvature given by the radius of curvature of the probing tip, R . The inverted SPM profile resembles more closely to the real surface with the correct spacing between the holes. However, this procedure is not generally applicable (see text).

The Approach of the Tip to the Sample

Approach system needs to approach tip to sample from mm-distances within the piezo range ($<1\mu\text{m}$) smoothly ($< 1\text{nm}/1000\text{Hz}$, if approach done without probe-step-procedure)

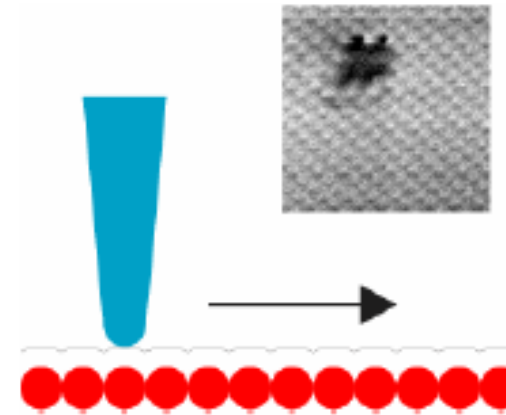
Piezo motors (can do steps from 20 nm to 1 μm)

Differential spring systems
or other mechanical reduction systems

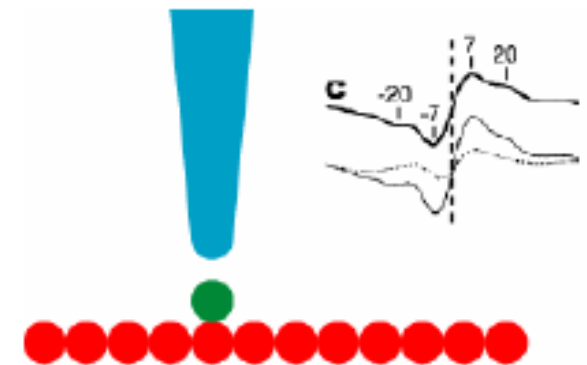


Different Principle Modes of SPM

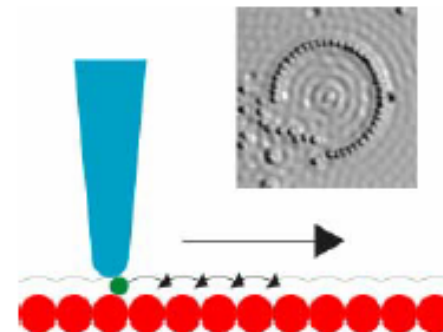
1. **Imaging** a “surface or surface properties” with high lateral (atomic) and vertical (pm) resolution. The tip-sample distance z adjusted to keep interaction constant or measurement of varying interaction at (controlled) z .



2. Local **spectroscopy** on selected sites. The interaction (i.e. tunneling current) is measured as a function of other parameters, i.e. tip-sample distance z or potential U_{tip} .

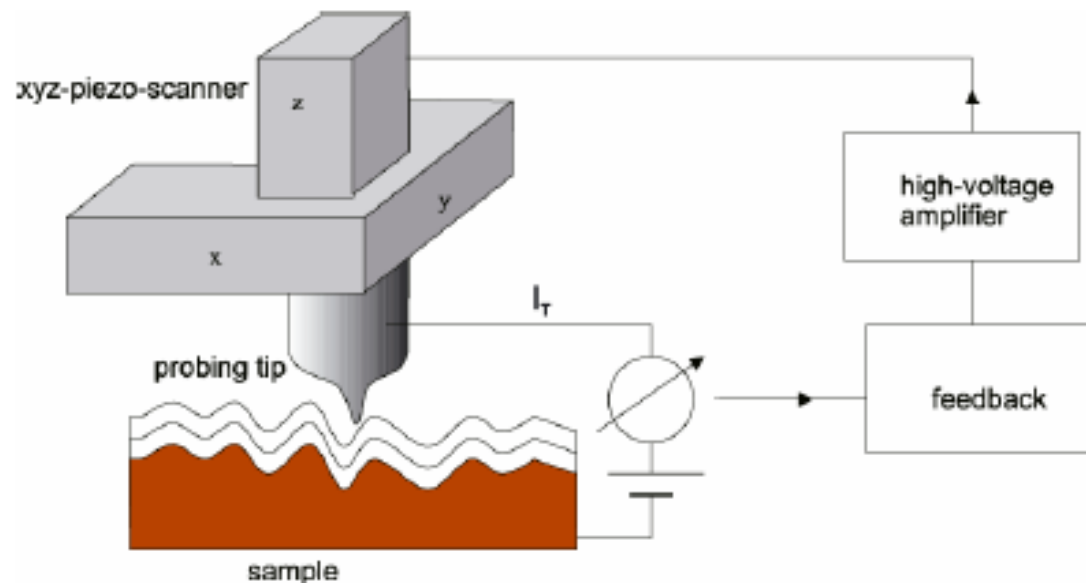


3. **Manipulation** of surface structures and surface states. Manipulation of atoms and molecules on surfaces. Transfer of atoms between tip and sample and vice versa. Lithography, deposition of charges, bleaching of fluorescing molecules



Tunneling: a Quantum Mechanical Effect

schematics of an STM

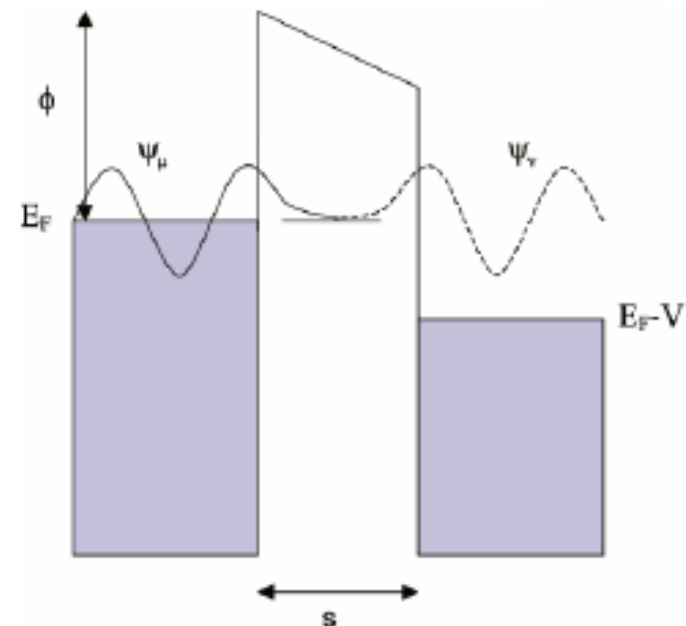


According to quantum mechanics, a particle with an energy E can penetrate a barrier $\phi > E$. In the classically forbidden region, the wave function ψ decays exponentially

$$\psi(z) = \psi(0)e^{-\frac{\sqrt{2m(\phi-E)}z}{\hbar}}$$

where m is the mass of the particle and $\hbar = 1.68 \cdot 10^{-34} \text{J}\cdot\text{s}$. In STM the barrier is given by the vacuum gap between sample and tip. Then, the tunneling current I_t can be calculated by taking into account the density of states of the sample at the Fermi edge:

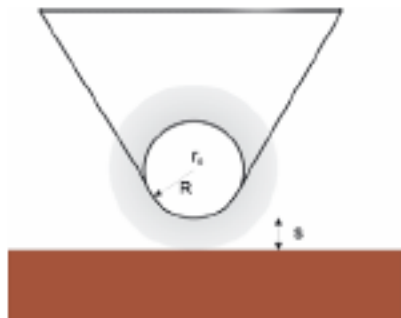
1d tunneling junction



$$I_t \propto V \rho_s(E_F) e^{-2 \frac{\sqrt{2m(\phi-E)}z}{\hbar}} \propto V \rho_s(E_F) e^{-1.025 \sqrt{\Phi} z}$$

where the barrier height Φ is in eV and z in Angstrom. **With a typical barrier height of $\Phi = 5 \text{ eV}$, which corresponds to the work function of gold, the tunneling current decays by an order of magnitude when the vacuum gap is changed by 0.1 nm !**

Tersoff-Hamann Model



Schematics of the Tersoff-Hamann model. The tip wave function is approximated by a s-wave. The tunneling current is proportional to the local density of states of the sample at the Fermi level, $\text{LDOS}(E_F)$, at the distance $r_0 = R + s$, which corresponds to the center of curvature of the tip.

The tunneling current between two electrodes, separated by an insulator, is given by with Fermi function:

$$I_t = \frac{4\pi e}{\hbar} \int_{-\infty}^{\infty} [f(E_F - eV + \varepsilon) - f(E_F + \varepsilon)] \times \rho_s(E_F - eV + \varepsilon) \rho_t(E_F + \varepsilon) M^2 d\varepsilon \quad f(E) = \frac{1}{1 + e^{(E - E_F)/k_B T}}$$

ρ_s, ρ_t are the density of states of sample and tip. The tunneling matrix element M is given by

$$M = \frac{\hbar}{2m} \int_{\text{surface}} \left(\psi_s^* \frac{\partial \psi_t}{\partial z} - \psi_s \frac{\partial \psi_t^*}{\partial z} \right) dS$$

where ψ_s, ψ_t are the wave functions of the sample and of the tip. For low voltages the integral simplifies to

$$I_t = \frac{4\pi e}{\hbar} \int_0^{eV} \rho_s(E_F - eV + \varepsilon) \rho_t(E_F + \varepsilon) M^2 d\varepsilon$$

In the case of a flat DOS tip, which means that ρ_t is constant in the studied energy range, the energy dependent part of the tunneling current is determined by the sample alone:

$$I \propto V \rho_s(E_F - eV)$$

which leads us again to the statement that the tunneling current is essentially determined by the LDOS of the sample at the Fermi energy.

Implementation in Different Environments

- ultra-high vacuum (UHV)

Most of the STM-work has been dedicated to UHV, because the preparation of conductive surfaces is often limited to this environment. Exceptions are gold, highly oriented pyrolytic graphite (HOPG) and other layered materials, such as transition metal dichalcogenide (e.g., TaS₂), which can be measured in ambient pressure.

- ambient pressure

- liquids

Active fields of applications are electrolytes and low current STM on organic molecules.

- low temperatures

At low temperature, the diffusion of atoms is reduced, which gives the opportunity to manipulate single physisorbed atoms [1]. Alternatively, high temperature gives the opportunity to observe dynamical processes [2, 3]. Room temperature experiments are sometimes disturbed by temperature variations, which lead to thermal drift.

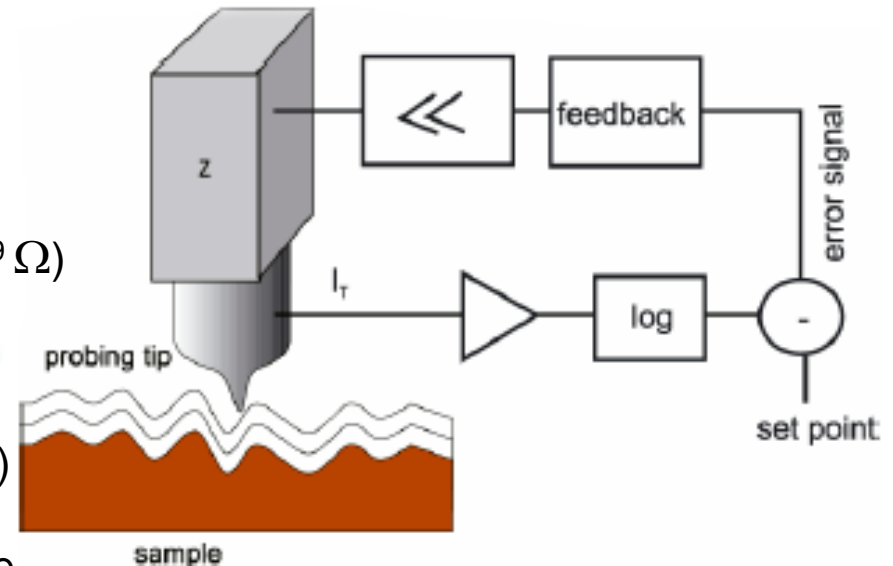
Refs.: [1] D. Eigler, E. Schweizer, Nature 344, 524 (1990)

[2] T. Linderoth, S. Horch, et al, Phys. Rev. Lett. 82, 1494 (1999),

[3] M. Hoogeman, D.G. van Loon et al., Rev. Sci. Instr. 69, 2072 (1998)

Operation Modes

- constant current mode or in the
- constant height mode
- various spectroscopic modes
- preamplifier:
gain selected from 10^8 to 10^9 by feedback resistor (10^8 - $10^9 \Omega$)
- current depends exponentially on tip-sample distance:
use logarithmic amplifier to linearize signal
- usually a PI-feedback is used:
error signal (difference between actual value and set-point)
is multiplied by a proportional gain (P-part) and integrated
(I-part) with a characteristic time constant. P- and I- part are
added together. The output of the feedback is then amplified and directly fed to the z-piezo.



Ziegler-Nichols procedure:

- increase P-part until small oscillations of the current are observed.
- reduce P-part to $0.45P_{krit}$
- measure oscillation period (T_{krit}) and set I-part to $0.85T_{krit}$

The output of the feedback loop is digitized and gives the "topography" image, $z(x,y)$. But attention: contours of constant tunneling current are not identical with the contours of constant total charge density, which would be the ideal topography of a surface, but is related to contours of constant local density of states at the Fermi level (LDOS). Atomic scale images often depend on the applied voltage, because of the variations of LDOS. Nevertheless, the constant current images are often very close to topography on a scale of some nanometers, where LDOS variations are small. Thus, step heights are relatively easy to be interpreted. Be aware of inhomogeneous surfaces!

Does an STM measure topography?

Generally

it is said that the movement of the tip at constant tunneling current or constant force reveals the topography of the sample surface.

But:

the STM records a map of constant density of states, which may differ from the geometric topography. For example, a molecule adsorbed on top of a metal surface may reduce the local density of states and may actually be imaged as a depression.

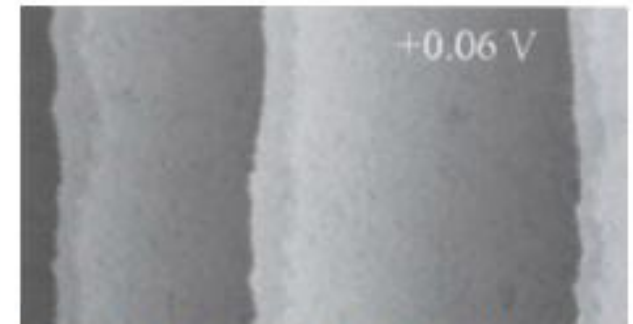
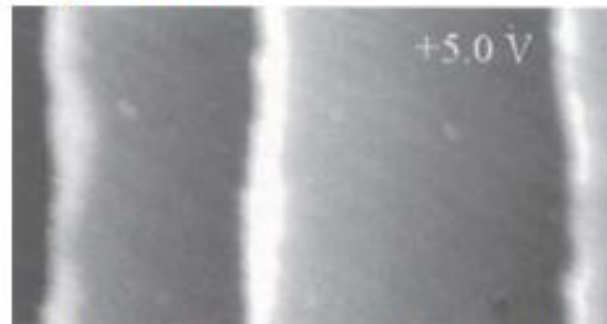
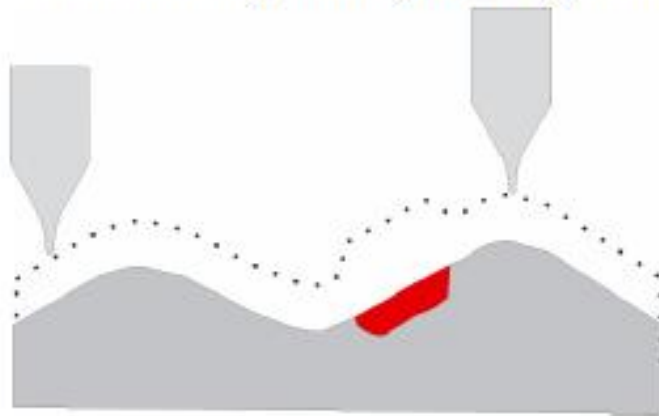


Image of Cu nanowire running along a step of Mo(11), recorded with different bias voltages. An image state produces a strong contrast (left) [1].

In scanning force microscopy, the situation is even more complicated as different parts of the tip interact differently with features on the surface. The measured height of steps, for example, may deviate strongly from their geometric height.

However:

on homogenous surfaces SPM measurements come as close to the real topography as possible with current experimental methods.